OncoImmunology 3:9, e955331; October 1, 2014; © 2014 Taylor & Francis Group, LLC

Tumor stroma-derived factors skew monocyte to dendritic cell differentiation toward a suppressive CD14$^+$ PD-L1$^+$ phenotype in prostate cancer

Lisa K Spary, Josephine Salimu, Jason P Webber, Aled Clayton, Malcolm D Mason, and Zsuzsanna Tabi*

Institute of Cancer and Genetics; School of Medicine; Cardiff University; Whitchurch, Cardiff, UK

Keywords: antigen cross-presentation, CCL2, dendritic cells, IL-6, immunosuppression, PD-L1, STAT3, tumor microenvironment, tumor stroma

Abbreviations: α-SMA, α-smooth muscle actin; CCL2, (C—C) motif chemokine ligand-2; CFSE, carboxyfluorescein succinimidyl ester; CK, cytokeratin; CM, conditioned media; CXCL, chemokine (C—X—C) motif; DC, dendritic cell; ELISA, enzyme-linked immunosorbent assay; GM-CSF, granulocyte macrophage colony-stimulating factor; HFF, human foreskin fibroblast; HGF, hepatocyte growth factor; IFN, interferon; IL, interleukin; IP-10, interferon-γ induced protein 10; I-TAC, interferon-inducible T cell α chemoattractant; LPS, lipopolysaccharide; MIF, macrophage inhibitory factor; prostate cancer; PBMC, peripheral blood mononuclear cells; PCaEp, prostate cancer epithelia; PCaSt, prostate cancer stroma; PD-1, programmed cell death-1; PD-L1, programmed cell death ligand-1; RANTES/CCL5, regulated on activation, normal T cell expressed and secreted; SCBM, stromal cell basal media; sDC, DC generated in the presence of 50% PCaSt-CM; SDF-1, stromal-derived factor-1; STAT3, signal transducer and activator of transcription 3; TIL, tumor infiltrating leukocytes; TGFβ, transforming growth factor β; VEGF, vascular endothelial growth factor.

Tumor-associated stromal myofibroblasts are essential for the progression and metastatic spread of solid tumors. Corresponding myeloid cell infiltration into primary tumors is a negative prognostic factor in some malignancies. The aim of this study was to define the exact role of stromal myofibroblasts and stromal factors in early prostate carcinoma (PCa) regulating monocyte infiltration and differentiation into dendritic cells (DCs). Epithelial and stromal primary cultures were generated from PCa biopsies and their purity confirmed. Stromal cells produced significantly more of the (C—C) motif chemokine ligand 2 (CCL2), interleukin 6 (IL-6) and transforming growth factor β (TGFβ) than epithelial cells. Monocyte chemoattraction was predominantly due to stromal-derived factors, mainly CCL2. DCs generated in the presence of stromal (but not epithelial) factors upregulated CD209, but failed to downregulate the monocyte marker CD14 in a signal transducer and activator of transcription 3 (STAT3)-dependent manner. Monocytes exposed to stromal factors did not produce detectable amounts of IL-10, however, upon lipopolysaccharide stimulation, stromal factor generated dendritic cells (sDC) produced significantly more IL-10 and less IL-12 than their conventional DC counterparts. sDC failed to cross-present tumor-antigen to CD8$^+$ T cells and suppressed T-cell proliferation. Most importantly, sDC expressed significantly elevated levels of programmed cell death ligand-1 (PD-L1) in a primarily STAT3 and IL-6-dependent manner. In parallel with our findings *in vitro*, tumor-infiltrating CD14$^+$ cells *in situ* were found to express both PD-L1 and CD209, and a higher percentage of tumor-associated CD3$^+$ T cells expressed programmed cell death-1 (PD-1) molecules compared to T cells in blood. These results demonstrate a hitherto undescribed, fundamental contribution of tumor-associated stromal myofibroblasts to the development of an immunosuppressive microenvironment in early PCa.

Introduction

A complex stromal network consisting of activated fibroblasts, immune cells, blood vessels and extracellular matrix support epithelial tumor development. The interactions between the different stromal components are necessary for tumor growth and cancer cell survival, in part by enabling tumor cells to evade immune recognition, a recognized hallmark of cancer.[1] This study seeks to elucidate how soluble factors produced by prostate cancer (PCa) tumor-associated fibroblasts contribute to local immune inhibitory mechanisms, focusing on their effect on dendritic cell (DC) differentiation. PCa is an inherently immunogenic cancer, as evidenced by a positive correlation between the frequency of CD8$^+$ tumor-infiltrating T-cells and prostate specific antigen recurrence-free survival.[2] A variety of immunotherapeutic approaches are being developed to target PCa, with the majority of trials conducted in metastatic PCa.[3] In the case of advanced disease, the tumor environment is considered to be

*Correspondence to: Zsuzsanna Tabi; Email: tabiz@cardiff.ac.uk
Submitted: 04/16/2014; Revised: 07/22/2014; Accepted: 07/25/2014
http://dx.doi.org/10.4161/21624011.2014.955331

highly immunosuppressive.[4] However, the developmental process giving rise to the immunosuppressive microenvironment at the primary site and the individual role of epithelia and stroma in contributing to this phenomenon have not been well studied. This is possibly due to the relative difficulty of generating sufficiently pure primary cell cultures[5] and the dominance of studies employing a limited number of established PCa cell lines of metastatic origin.

A diverse range of myeloid cells that produce anti-inflammatory cytokines and display immunosuppressive functions infiltrate prostate tumors, including monocytes, macrophages that can be type-1, or -2 polarized (M1 and M2, respectively) and myeloid-derived suppressor cells (MDSCs).[6-10] $CD68^+$ myeloid cells in PCa tissue were found to localize in the stroma in low grade cancer whereas these monocytes were found dispersed throughout the tissue in high grade PCa,[11] indicating both an early and sustained role for these cells throughout tumor progression. Myeloid cell infiltration into malignant tissues has been shown to result from chemoattraction mediated by (C—C) motif chemokine ligand (CCL2) and stromal-derived factor-1 (SDF-1/CXCL12).[12,13] While both stromal and epithelial cells can release these chemokines,[13,14] the exact contribution of the different cellular components to myeloid cell chemoattraction has not been studied in primary PCa. There is also little information available about the role of stroma in early PCa contributing to the development of myeloid-derived DCs. We examined the effects of soluble factors derived from primary PCa epithelial cells (PCaEp) and stromal cells (PCaSt) on monocyte attraction and differentiation into DCs as well as the function of stromal-conditioned DC. We show that PCaEp have minimal chemoattraction for myeloid cells while PCaSt-derived factors efficiently attract monocytes in a predominantly CCL2-mediated manner. PCaSt also drastically skews monocyte-DC differentiation, resulting in cells that retain CD14 surface expression and significantly upregulate the expression of the inhibitory marker programmed cell death ligand-1 (PD-L1). These $CD14^+$ DC are immunosuppressive and incapable of cross-presenting tumor antigen to T cells. The immune regulatory effect of PCaSt-derived factors is mediated via the rapid activation of the signal transducer and activator of transcription-3 (STAT3) pathway in granulocyte macrophage colony-stimulating factor (GM-CSF) and interleukin (IL-4) treated monocytes. Our results provide compelling evidence that tumor-associated stromal fibroblast factors significantly affect the generation of immunosuppressive DCs that aid in PCa immune evasion. These conclusions point toward the importance of targeting not only carcinoma cells but stromal cells as well in PCa in order to improve clinical outcome.

Results

Development of PCa-derived primary epithelial and stromal cell cultures

The majority of *in vitro* PCa studies utilize the cell lines LNCaP, DU145 and PC3. These were derived from metastatic lesions decades ago and are thus unlikely to represent the primary tumor site.[5] To better understand the primary PCa environment, we established epithelial (PCaEp) and stromal (PCaSt) primary cultures from fresh PCa biopsies by plating dissociated cells in distinct culture media. Morphologically, PCaEp appeared rounded, forming cobblestone-like monolayers, whereas stromal cells displayed a fibroblast-like morphology (**Fig. 1A**). The absence of α-smooth muscle actin (α−SMA) in the PCaEp and of cytokeratin (CK) in the PCaSt preparations demonstrated the purity of these cultures (**Fig. 1A**). CK5/CK14 expression studies with a sensitive europium-based detection method suggested a low level of basal marker expression (2.5-fold increase of CK14 signal over isotype), consistent with relatively scarce basal epithelial cells in PCaEp cultures (**Fig. 1Bi**). The expression of luminal epithelial cell markers, CK8/CK18, confirmed heterogeneity of the PCaEp cultures (**Fig. 1Bii**). Levels of CK8/CK18 were lower in the PCaEp cells relative to DU145 cells, but similar to that detected in LNCaP cells (**Fig. 1Bii**). No expression of α-SMA was detected in PCaEp cultures confirming that no contaminating PCaSt cells were present (**Fig. 1A, Biii**). Prostate stroma has been identified by expression of vimentin and α-SMA.[15] Vimentin expression levels in the PCaSt were consistent with those observed in human foreskin fibroblasts (HFF) (**Fig. 1Ciii**), suggesting PCaSt are of mesenchymal origin. Presence of α-SMA was also observed in PCaSt (**Fig. 1A, Ciii**), consistent with a myofibroblastic phenotype. To detect potential epithelial cell contamination, the CK markers were analyzed and to detect potential smooth muscle cell contamination, analysis of the marker Desmin[15] was included. PCaSt and HFF cells were both negative for cytokeratins, confirming the absence of epithelial cell contamination (**Fig. 1Ci, ii**), while the lack of Desmin indicates no contaminating smooth muscle cells (**Fig. 1Ciii**). These data provide evidence that the stromal and epithelial primary cultures are morphologically and histologically distinct.

PCa-derived primary PCaEp and PCaSt have distinct cytokine profiles

Determining the cytokine profile of both PCaEp and PCaSt is essential for understanding the influence they can have on immune cell infiltration in the tissue. Having normalized for cell number, a cytokine array revealed that while IL-8, chemokine (C—X—C) motif ligand 1 (CXCL1), endothelial plasminogen activator inhibitor E1 (SERPIN)-E1 (also known as plasminogen activator inhibitor 1 (PAI-1)) and macrophage migration inhibitory factor (MIF) were released at relatively high levels by both cell types, notable differences were observed for the production of several factors (**Fig. 2A, B**). PCaEp cell cultures produced high levels of GM-CSF, IL-1, IL-1 receptor antagonist (IL-1Ra), interferon-γ-induced protein 10 (IP-10 or CXCL10), IFNγ and interferon-inducible T cell α chemoattractant (I-TAC or CXCL11) in comparison to PCaSt cultures (**Fig. 2B**). In contrast, PCaSt robustly produced CCL2 and somewhat higher levels of IL-6, (C—C) motif chemokine ligand 5 (RANTES or CCL5), CD54, IL-13 and IL-17, than their PCaEp cell counterparts (**Fig. 2B**). Analysis of transforming growth factor β (TGFβ) by enzyme-linked immunosorbent assay (ELISA) demonstrated that PCaSt produced >8 times more TGFβ compared

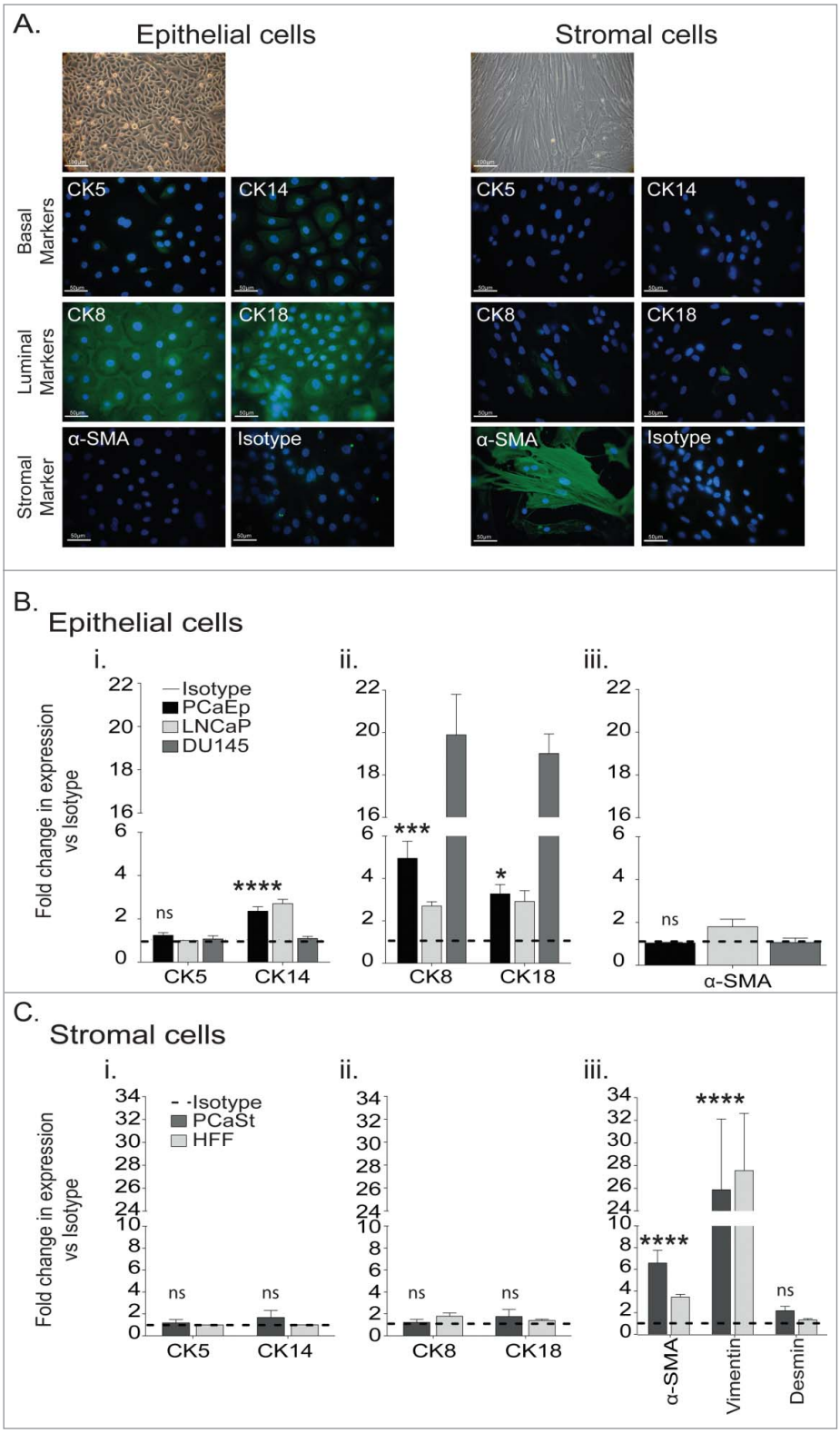

Figure 1. Characterization of prostate cancer-derived epithelial and stromal primary cultures. Primary prostate tumor specimens were dissociated and cells plated in epithelial or stromal cell media to derive prostate epithelial (PCaEp) or prostate stromal (PCaSt) cell cultures. Cells were stained using antibodies against the indicated markers and immunofluorescent detection and microscopy (**A**) or Europium-based detection was carried out to quantify the relative expression level of the indicated markers (**B** and **C**). (**A**) Phase contrast (20X; bar = 100 μm, top image) and immunofluorescent imaging (40X; bar = 50 μm) of epithelial (left) and stromal (right) cells at passage 2. Epithelial cells were identified using markers cytokeratin (CK) 5, 8, 14 and 18, whereas α-smooth muscle actin (α-SMA) was used to identify stromal cells. (**B** and **C**) Relative expression levels of markers using DELFIA® Europium-based detection method. Dotted lines represent the isotype controls. (**B**) Mean+SEM of expression of basal markers CK5/14 (**i**), luminal markers CK8/18 (**ii**) and α-SMA (**iii**) in epithelial (PCaEp) cultures, calculated from the means from triplicates for 8 donor biopsies and from PCa cell lines LNCaP and DU145 (triplicates), as indicated. (**C**) Mean+SEM of CK5/14 (**i**), CK8/18 (**ii**) and Vimentin and α-SMA (**iii**) expression in stromal (PCaSt) cultures, calculated from 11 donor biopsies and human foreskin fibroblasts (HFF) calculated from triplicates samples. Statistical analysis was performed by unpaired Student's t-test; $^{****}p < 0.0001$, $^{***}p < 0.001$, $^{**}p < 0.01$, $^{*}p < 0.05$.

with PCaEp cell cultures derived from the same biopsy (**Fig. 2C**). Further ELISA of the cytokines produced by PCaSt versus PCa cell lines (DU145 or PC3) or human foreskin fibroblast (HFF) confirmed secretion of relatively higher levels of hepatocyte growth factor (HGF) but relatively lower levels of vascular endothelial growth factor (VEGF) and stromal cell derived factor-1 (SDF-1). Taken together, the results indicate that PCa stroma is the primary producer of CCL2 and IL-6 with potential regulatory effects on myeloid cells.

PCaSt are more chemoattractive to monocytes than PCaEp

To elucidate the chemoattractive potential of primary PCaEp- and PCaSt-derived soluble factors, monocytes were migrated for 4 h toward conditioned media (CM) from epithelial (PCaEp-CM) or stromal cells (PCaSt-CM), respectively, and counted. The serum-free PCaEp media alone supported no spontaneous monocyte migration and migration was not induced even when 50% CM was added (**Fig. 3A**). PCaSt media alone supported some spontaneous migration of monocytes (2–18%); in addition, stroma CM was highly

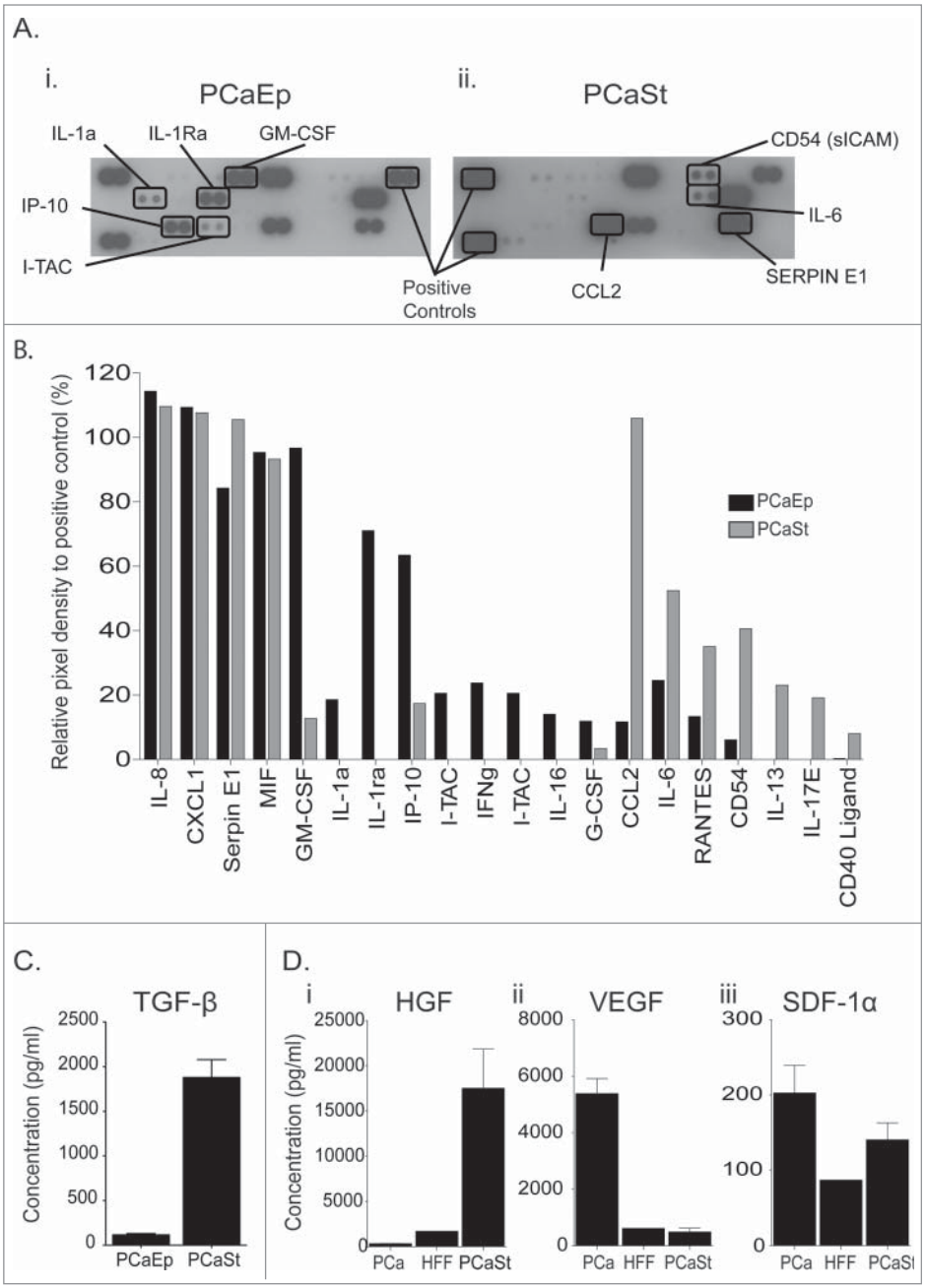

Figure 2. The cytokine profiles of prostate cancer-derived primary epithelial and stromal cultures. Secreted cytokines from the distinct cultures obtained from primary prostate tumor cells cultured in epithelial versus stromal selective media were analyzed via a cytokine array (**A and B**) and ELISA (**C and D**). (**A**) Scanned images of cytokine arrays from conditioned media obtained from epithelial (PCaEp) (**i**) and stromal (PCaSt) cultures. (**ii**). Highlighted are proteins that are significantly up- or downregulated. (**B**) Densitometry of cytokine array was carried out using ImageJ software and data was normalized to the average value of the positive controls. Mean relative percentages of image densities, calculated from 3 autologous pairs of conditioned media from PCaEp (black) and PCaSt (gray) cultures are shown. (**C**) Transforming growth factor β (TGFβ) ELISA from conditioned media derived from PCaEp and PCaSt cultures. Mean+SEM of TGFβ concentrations are shown from triplicate analysis of 3 primary cultures each. Results are normalized for cell numbers. (**D**) Mean + SEM of growth factor concentrations of hepatocyte growth factor (HGF) (**i**), vascular endothelial growth factor (VEGF) (**ii**) and stromal-derived factor-1α (SDF-1α) (**iii**), determined by ELISA from conditioned media of PCaSt cultures, normalized for cell numbers, calculated from triplicate samples from 3 primary cultures. The levels in PCa cell lines (DU145 or PC3) and human foreskin fibroblasts (HFF) calculated from triplicate samples are shown for comparison.

chemoattractive, triggering a 2-3 fold increase in monocyte migration toward PCaSt-CM in a dose-dependent manner from all donors studied (**Fig. 3A**). We evaluated the regulation of monocyte migration by CCL2 using recombinant CCL2. Increased numbers of monocytes migrated at all concentrations studied, with the effects of 0.01 and 0.1 ng/mL being significant ($p < 0.01$; **Fig. 3B**). CCL2 concentrations produced by 3 different PCaEp cultures varied between 0.05–0.1 ng/mL while in 4 different PCaSt cultures, CCL2 concentrations varied between 2–15 ng/mL (**Fig. 3C**), suggesting that CCL2 levels in PCaSt-CM are sufficiently high to regulate monocyte migration. In order to determine the tumor-specificity, the levels of CCL2 in the CM from PCaSt cultures were compared to the levels in CM derived from stroma collected from biopsies of normal adjacent areas (St-CM) of the prostate (autologous biopsy pairs). Significantly increased CCL2 concentrations were found in tumor-derived vs. normal stroma-derived CM from 2 out of 4 biopsies (**Fig. 3C**). Finally, to assess how much of the chemoattraction in PCaSt-CM is CCL2-mediated, CCL2 was neutralized using a blocking antibody (2 μg/mL). The percentage of monocytes that migrated in the presence of blocking antibody was significantly reduced in both donors, by 88% and 85% respectively, when compared to the CM-free control (**Fig. 3D**), confirming that stromally produced CCL2 is largely responsible for the regulation of monocyte migration into the tumor.

PCaSt-CM alters DC differentiation

Studies in prostate, colorectal, breast, renal cell and pancreatic carcinomas have indicated that the presence of myeloid cells in the tumor tissue correlates with an unfavorable prognosis.[10,16-19] However, relatively little is known about the immunologic

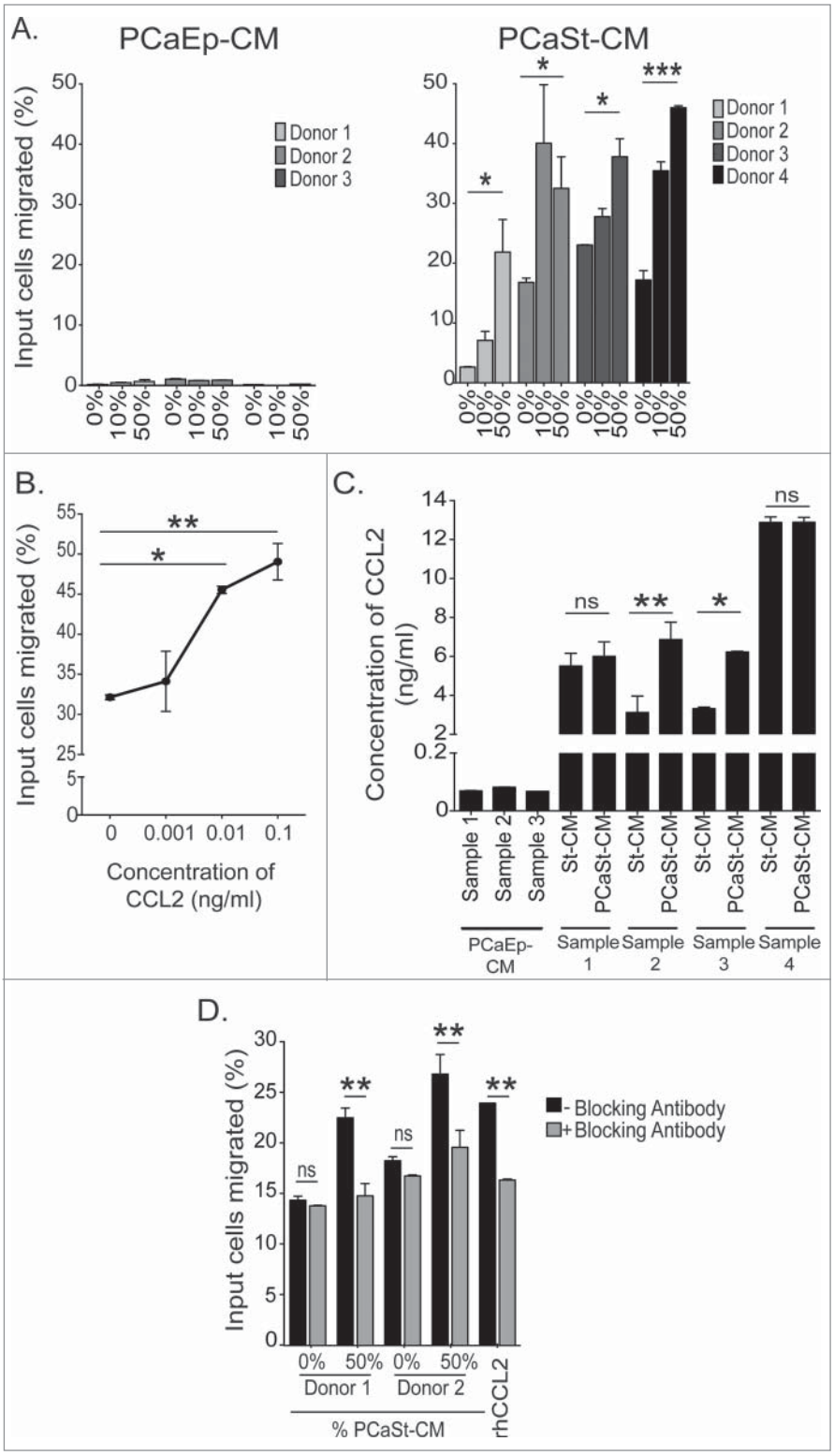

Figure 3. Monocytes are chemoattracted by stromal cell-derived chemokine CCL2. Conditioned culture media from primary prostate tumor epithelial or stromal-derived cell cultures were analyzed for their abilities to stimulate migration of monocytes. (**A**) The percentage of input monocytes that migrated toward 0–10–50% conditioned media either from prostate cancer epithelial cultures (PCaEp-CM) (3 donors; left panel), or from prostate cancer stromal cultures (PCaSt-CM) (4 donors; right panel). Each bar represents the mean + SEM of the percentage of migrated monocytes from 6 replicates (duplicates of 3 independent PCaEp-CM or PCaSt-CM, respectively). (**B**) Percentage of input monocytes that migrated in the presence of recombinant (C-C) motif chemokine ligand 2 (CCL2) at the indicated concentrations (0, 0.001, 0.01 and 0.1 ng/mL) (mean + SEM of triplicates). (**C**) CCL2 concentrations in 3 independent PCaEp-CM and in CM from normal (St-CM) and tumor (PCaSt-CM) cultures generated from 4 different biopsies (mean + SEM of triplicates each). (**D**) Monocyte migration from 2 healthy donors in the presence (gray) or absence (black) of 2 μg/mL CCL2 neutralizing antibody. Bars represent the mean + SEM of the percentage of migrated monocytes toward PCaSt-CM from 6 replicates (duplicates of 3 independent PCaSt-CM). Recombinant human (rh) CCL2 was used at 0.1 ng/mL as a control. Statistical analysis was performed by two-way ANOVA; $^{****}p < 0.0001$, $^{***}p < 0.001$, $^{**}p < 0.01$, $^{*}p < 0.05$.

behavior of these cells. In order to characterize the effects of PCaSt on monocyte-to-DC differentiation, DCs were generated with GM-CSF and IL-4 in the presence of 50% PCaSt-CM. The resulting DCs (referred to as sDC in this paper) remained $CD14^+$ on day 5 (**Fig. 4A**). The proportion of $CD14^-/CD209^+$ cells developed in the presence of PCaSt-CM was significantly reduced in all donors tested, demonstrating a robust inhibition of DC differentiation (**Fig. 4B**). Compared with the effects of PCaSt-CM, normal stroma-derived CM inhibited CD14 downregulation during DC differentiation at a lesser extent than PCaSt-CM, however this difference did not reach significance. (**Fig. 4C**). Further characterization of the PCaSt-CM-induced $CD14^+CD209^+$ cells confirmed that these cells displayed a $CD14^+/CD68^+/CD16^+/CD15^-/CD124^+$ phenotype (**Fig. 4Di, ii**). These results suggest that stroma-derived factors override monocyte-DC differentiation in the presence of DC-differentiating cytokines, GM-CSF and IL-4, leading to a semi-mature DC phenotype. Some markers expressed by these cells have also been identified in MDSC panels, suggesting a skewing toward immunosuppression.

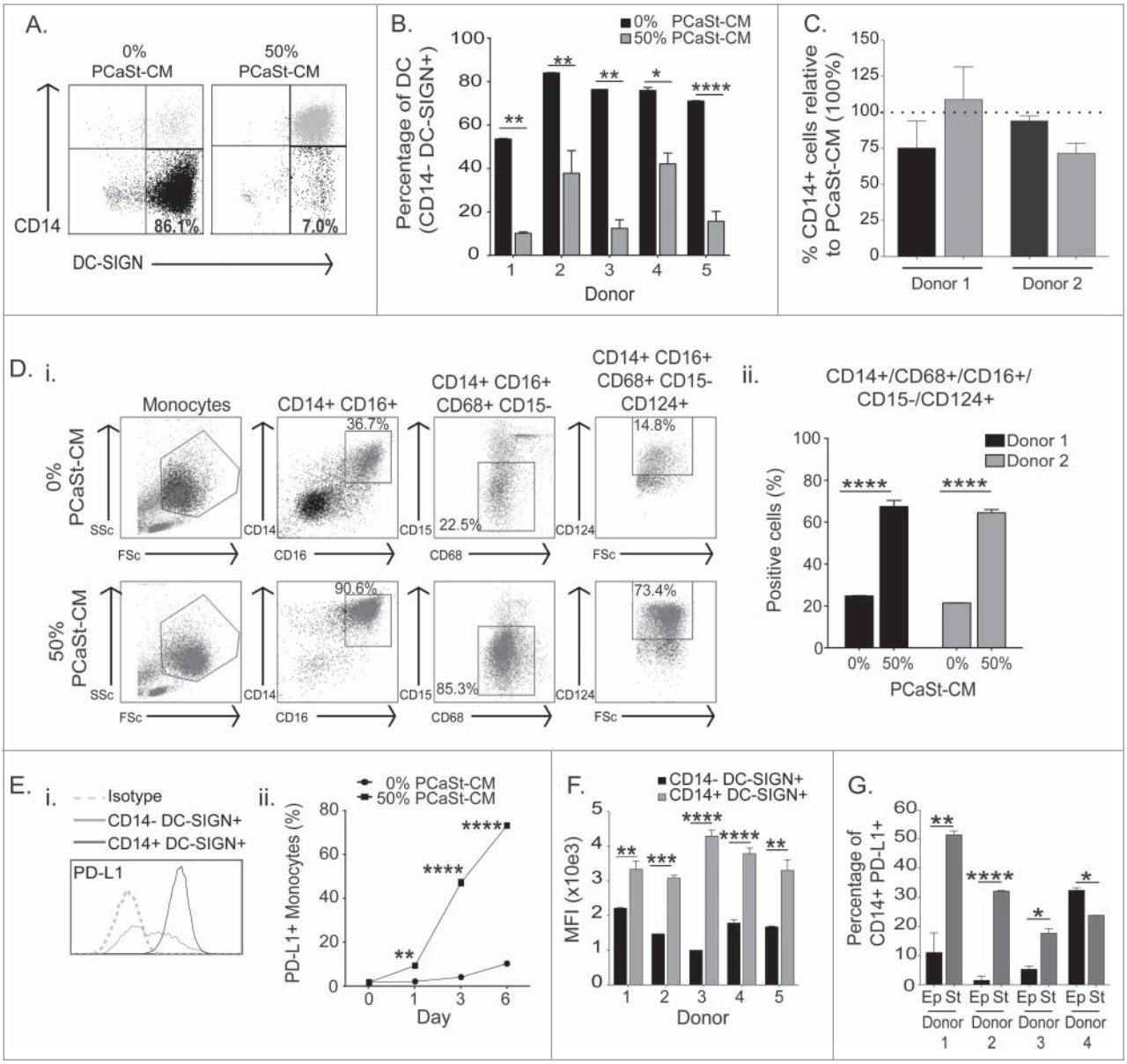

Figure 4. Conditioned media from prostate cancer stromal cells inhibits dendritic cell differentiation. Conditioned culture media from primary prostate tumor epithelial (PCaEp-CM) or stromal (PCaSt-CM) cell cultures were analyzed for their abilities to inhibit monocyte differentiation to dendritic cells (DCs). Monocytes stimulated with 50 ng/mL GM-CSF and 500 U/mL IL-4 in the presence or absence of 50% PCaSt-CM or PCaEp-CM were monitored for DC differentiation (downregulation of CD14 and upregulation of CD209) by immunofluorescence staining and flow cytometry. (**A**) Representative dot-plots for CD14 and CD209 expression on DCs cultured in the absence (DC; first dot plot) or presence of 50% PCaSt-CM (sDC) from 3 independent primary cultures (sDC1–3) as indicated. The numbers demonstrate the percentages of $CD14^{-}CD209^{+}$ cells. (**B**) Summary of the phenotype of day 5 DC (black) or sDC (gray) from 5 healthy donors. Bars represent the mean + SEM of the percentage of $CD14^{-}CD209^{+}$ cells. PCaSt-CM treatment was carried out in duplicates with 3 independent PCaSt-CM, and in triplicates without PCaSt-CM. (**C**) DCs were generated from monocytes from 2 healthy donors in the presence of 50% of either PCaSt- or normal stroma-CM from 2 independent biopsies (1 = black, 2 = gray) and percentages of $CD14^{+}$ cells were analyzed by flow cytometry. Bars represent the relative mean percentage + SEM of $CD14^{+}$ cells generated with normal stroma CM in triplicates, compared to the values obtained with PCaSt-CM (dotted line, 100%). (**D**)(**i**) Representative dot-plots of the full phenotypic analysis of DCs generated in the absence (DC; first row of dot plots) or presence (sDC; second row of dot plots) of 50% PCaSt-CM. The gates highlight the cells in the phenotype group indicated above the dot plots. The percentage values refer to the monocyte gate as the parent gate. (**ii**) Percentages of $CD14^{+}/CD16^{+}/CD68^{+}/CD15^{-}/CD124^{+}$ cells present in DC or sDC generated from 2 healthy donors. Bars represent the mean + SEM of the percentage of cells with the above phenotype from triplicates for DC or 6 replicates (duplicates of 3 independent PCaSt-CM) for sDC. (**E**)(**i**) Representative histogram of programmed cell death ligand-1 (PD-L1) expression on DCs treated with 0% (DC) or 50% PCaSt-CM (sDC). (**E**)(**ii**) Flow cytometry analysis indicating time-dependent upregulation of PD-L1 on DC or sDC. Mean + SEM of % $PD\text{-}L1^{+}$ cells from triplicate cultures are shown. (**F**) Summary of PD-L1 expression on day 5 DC (black) or sDC (gray) generated from 5 healthy donors, (the latter with 3 independent PCaSt-CM). Mean + SEM of PD-L1 expression levels as reported by mean fluorescence intensity (mfi) from triplicates are shown. (**G**) Percentages of $CD14^{+}$ $PD\text{-}L1^{+}$ cells generated from 4 healthy donors in the presence of 50% PCaEp-CM (Ep – black bars) and 50% PCaSt-CM (St – gray bars) derived from one biopsy. Mean + SEM of $CD14^{+}PD\text{-}L1^{+}$ (percentage positive cells) from triplicates are shown. Statistical analysis was performed by two-way ANOVA; $^{****}p < 0.0001$, $^{***}p < 0.001$, $^{**}p < 0.01$, $^{*}p < 0.05$.

PCaSt-CM induces the upregulation of the immune checkpoint ligand PD-L1 on DCs

There are several mechanisms by which myeloid cells suppress antitumor immune responses, including via the inhibitory PD-1/PD-L1 pathway. PD-1 expression on T cells can be a sign of recent activation or exhaustion due to chronic stimulation, whereas PD-L1 is frequently expressed on tumor cells or tumor-infiltrating myeloid cells.[20] We tested whether PD-L1 expression is upregulated on sDC. Stromal conditioning induced a highly significant increase in PD-L1 expression on sDC (**Fig. 4Ei**). PD-L1 expression was significantly elevated already at 24 h after monocyte treatment with GM-CSF/IL-4 in the presence of 50% PCaSt-CM and its level continued to rise with time (**Fig 4Eii**). On day 7, PD-L1 expression was significantly elevated on sDC generated from all 5 donors studied (**Fig. 4F**). The percentage of $CD14^+$ $PD\text{-}L1^+$ cells, induced by PCaSt-CM was significantly higher in 3 out of the 4 donors than that induced by PCaEp-CM (**Fig. 4G**), confirming that soluble factors from PCaSt cells have a greater effect on monocyte differentiation than those secreted from PCaEp cells.

PCaSt-CM alters the cytokine profile and T-cell stimulatory function of DCs

To test the nature of DCs generated in the presence of PCaSt-CM, DCs were stimulated with lipopolysaccharide (LPS) and IL-12 and IL-10 cytokine levels were measured. DCs derived in the presence of PCaSt-CM produced significantly less IL-12 in response to LPS in comparison to DCs differentiated in the absence of conditioned media ($p < 0.001$; **Fig. 5A**) In contrast, IL-10 secretion was significantly elevated in LPS-stimulated DCs derived in the presence of PCaSt-CM ($p = 0.01$ **Fig. 5B**) compared to those DC generated in the absence of stromal CM, a response consistently observed among cells from all 3 donors studied. However, a time kinetics experiment of IL-10 production revealed that without LPS stimulation IL-10 production was low in both groups irrespective of their conditioned media treatment status and, that sDC actually produced less IL-10 than normal DCs on day 3 of the 4-day observation (**Fig. 5C**).

To evaluate the T-cell stimulatory functions of sDC, we first performed an allogeneic T-cell stimulation in a mixed lymphocyte reaction (MLR) experiment. After 3 d, T-cell proliferation was significantly lower in cultures stimulated by sDC when compared to normal DCs (**Fig. 5D**). To determine if sDC were in fact inhibitory toward T cells, T-cell proliferation was induced by T cell receptor cross-linking using anti–CD3-CD28 antibody-coated beads in the presence of autologous sDC. T-cell proliferation was significantly inhibited by sDC at 1:20 and 1:10 DC:T cell ratios (**Fig. 5E**). In order to determine the antigen processing and presentation capability of sDC, these cells were employed to crosspresent a complex tumor antigen (5T4-oncofetal antigen[21]) to 5T4-specific $CD8^+$ T cells. IFNγ production by T cells was significantly lower after stimulation with sDC, in comparison to normal DCs, both loaded with the 5T4 protein ($p < 0.01$; **Fig. 5F**). In order to prove that the lack of antigen cross-presentation was not due to impaired antigen uptake, the phagocytic ability of DCs was studied via the uptake of carboxyfluorescein succinimidyl ester (CFSE)-labeled, irradiated DU145 PCa cells (**Fig. 5Gi**). The percentage of phagocytic, $HLA\text{-}DR^+$ cells was significantly elevated in sDC in comparison to the control ($p < 0.01$; **Fig. 5Gii**) indicating that it is antigen processing and not antigen uptake by DCs that is affected by stromal factors.

PCaSt-CM activates the STAT3 pathway in monocytes

The cytokines produced preferentially by PCaSt, especially IL-6 (**Fig. 2B**), point toward a likely stimulation of the STAT3 pathway in sDC. To determine the activation status of STAT3 by stromal cytokines, monocytes were treated with 50% PCaSt-CM plus GM-CSF/IL-4 and STAT3 phosphorylation of the tyrosine (Y705) and serine (S727) residues was analyzed 10 min later. Phosphorylation of both residues was observed (**Fig. 6Ai, Bi**) and they were highest at 5–10 min but still detectable 60 min after treatment, especially at the S727 residue (**Fig. 6Aii, Bii**). To establish if blocking STAT3 phosphorylation would prevent the development of the sDC phenotype described earlier, a STAT3 inhibitor (Cpd188) was added (0.5–10 μM) to monocytes for 1 h prior to treatment with PCaSt-CM and GM-CSF/IL-4. Day 5 DC generated in the presence of 50% PCaSt-CM and 5 and 10 μM of the STAT3 inhibitor were phenotypically comparable to DC generated in the absence of PCaSt-CM (**Fig. 6Ci**), as CD14 expression was significantly downregulated on these cells (**Fig. 6Cii**).

PD-L1 upregulation is prevented by STAT3 inhibition

During the course of these studies, we observed that in addition to attenuating the development of stroma-induced $CD14^+$ DC (**Fig. 6Cii**), STAT3 blockade also significantly inhibited PD-L1 upregulation on sDC (**Fig. 6Di**) in 2 out of 3 donors (**Fig. 6Dii**). In order to identify individual cytokines in PCaSt-CM, responsible for observed PD-L1 upregulation, we studied the effect of IL-6 and IL-10 blocking antibodies on PD-L1 expression levels on sDC. IL-6 blocking antibody, applied together with 50% PCaSt-CM, partially inhibited PD-L1 upregulation (**Fig. 6E**). Although IL-10 has been implicated in PD-L1 upregulation,[22] we did not detect significant IL-10 levels in the PCaSt-CM via cytokine array analysis (data not shown) or in the supernatant of sDC developing in the presence of 50% PCaSt-CM (**Fig. 5C**). Indeed, IL-10 neutralizing antibody had a much smaller inhibitory effect on stroma-mediated PD-L1 upregulation than that observed with the IL-6 neutralizing antibody (**Fig. 6E**). Furthermore, synergistic effect between IL-10 and IL-6 blocking was not observed. The results suggest that stromal IL-6 in PCa is a main driver of PD-L1 upregulation on myeloid cells.

$CD14^+CD209^+PD\text{-}L1^+$ tumor-infiltrating leukocytes

In order to confirm the significance of our observations *in vivo*, tumor biopsies were first tested for the presence of tumor-infiltrating leukocytes (TIL). In malignant tissues, unlike in tumor-free prostate tissue (**Fig. 7Ai**), areas of significant leukocyte infiltration were observed (**Fig. 7Aii**). Next, TIL isolated from the malignant biopsies were phenotyped by flow cytometry.

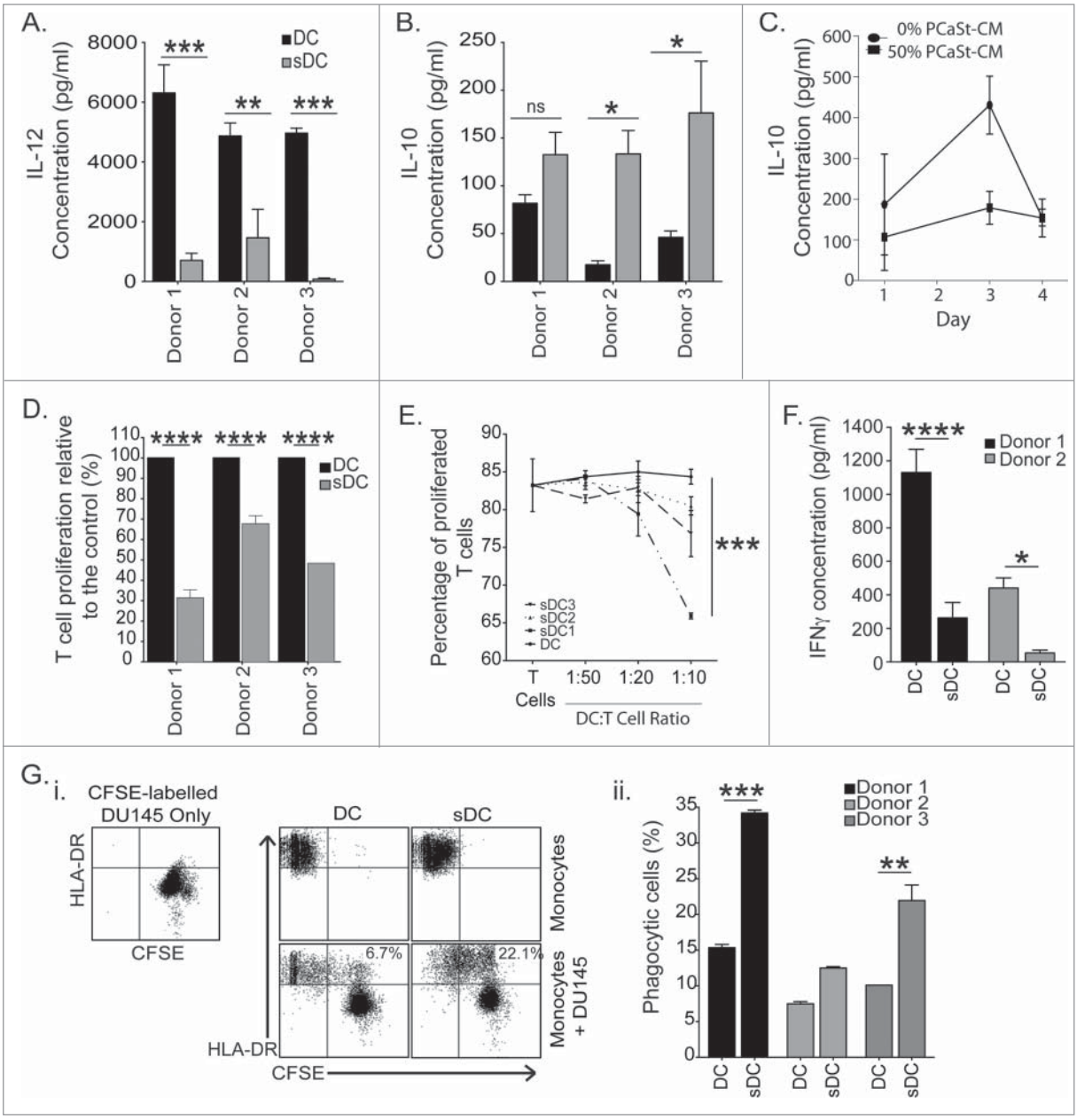

Figure 5. Stromal-derived factors generate immunosuppressive dendritic cells. **(A–B)** To test the nature of DCs generated in the presence of PCaSt-CM, DCs were stimulated with lipopolysaccharide (LPS) and IL-12 and IL-10 cytokine levels were measured. Supernatants of day 5 DC grown in the absence (DC) or in the presence of 50% prostate cancer stroma conditioned media (PCaSt-CM) (sDC) from 3 healthy donors were tested for IL-12 (**A**) and IL-10 (**B**) production 24 h after LPS stimulation. Bars represent the mean + SEM of the concentrations of cytokines. sDC were generated with 50% PCaSt-CM from 9 replicates (triplicates of 3 independent PCaSt-CM). (**C**) Time kinetics of IL-10 production by DC or sDC (as in **B**) without LPS treatment. Mean ± SEM of IL-10 concentrations from triplicate cultures are shown. **(D)** Mixed lymphocyte reaction to test the T-cell stimulatory functions of sDC. T cells were stimulated with allogeneic DC or sDC derived from 3 healthy donors. Bars represent the mean + SEM of the relative T-cell proliferation, where proliferation induced by DC represents 100%. sDC was generated with 50% PCaSt-CM from 6 replicates (duplicates of 3 independent PCaSt-CM). (**E**) T cell receptor cross linking experiment to test the inhibitory functions of sDC. sDC inhibit T cell proliferation induced by CD3-CD28 antibody-coated beads at varying ratios of sDC:T cells (x-axis). Proliferating T cells were defined by their CFSE dilution; sDC were generated by using 3 different PCaSt-CM. Mean + SEM from triplicate samples are shown. (**F**) Tumor antigen cross-presentation by DC and sDC to antigen-specific T-cells. Bars represent the mean + SEM of IFNγ (pg/mL) produced by T-cells following stimulation with DC or sDC loaded with 5T4 antigen, from 6 replicates (triplicates of 2 independent PCaSt-CM) after background IFNγ production (T cells alone) has been subtracted. (**G**)(**i**) Representative dot plots of phagocytosis of carboxyfluorescein succinimidyl ester (CFSE)-labeled irradiated DU145 cells by DC and sDC. Top row: cells before mixing: CFSE+HLA-DR- DU145 cells (first panel) or HLA-DR+CFSE- DC (second panel) and sDC (third panel). Lower row: DU145 cells added to DC (left) or sDC (right). The numbers indicate the percentage of phagocytic cells shown as double positive cells (upper right quadrants). (**ii**) Summary of phagocytosis from 3 healthy donors. Bars represent the mean ± SEM of double positive cells as shown in (**i**). sDC were generated with 50% PCaSt-CM from 4 replicates (duplicates of 2 independent PCaSt-CM). DC results were calculated from duplicates. Statistical analysis was performed by two-way ANOVA; ****$p < 0.0001$, ***$p < 0.001$, **$p < 0.01$, *$p < 0.05$.

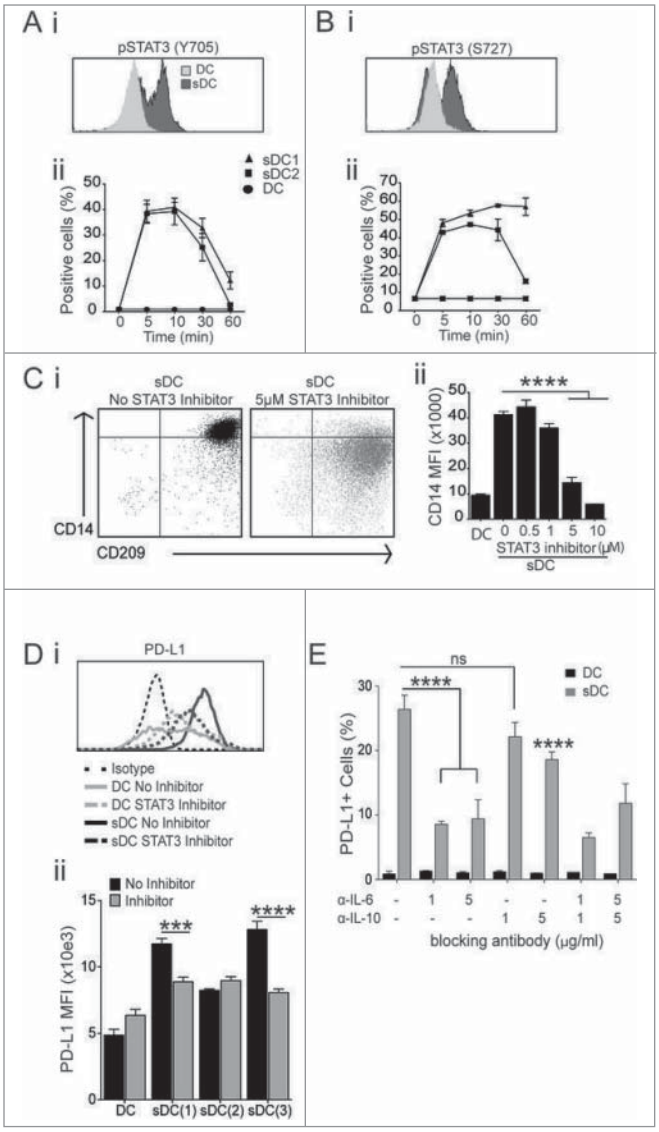

Figure 6. STAT3 and IL-6 blocking prevents altered DC differentiation caused by conditioned media from prostate cancer stroma. To determine the role of IL-6 and STAT3 in mediating responses to prostate cancer stroma conditioned media (PCaSt-CM), the phosphorylation status of STAT3 (**A–B**) and the effects of blockade of STAT3 and IL-6 signaling (**C-E**) were analyzed using monocytes treated with 50% PCaSt-CM plus GM-CSF/IL-4 with or without inhibitor, as indicated. (**A and B**) STAT3 (signal transducer and activator of transcription-3) phosphorylation (pSTAT3) was measured by flow cytometry. (**i**) Representative histograms showing pSTAT3 levels on the Y705 (**A**) or S727 residue (**B**). CD14+ cells were treated with GMCSF/IL-4 and exposed to 0% (DC) or 50% (sDC) conditioned medium from prostate cancer stromal cultures (PCaSt-CM) for 10 min. (**ii**) The mean ± SEM percentages of pSTAT3+ monocytes as in (**i**) after 0, 5, 10, 30 and 60 min (triplicates, sDC generated with 2 independent stromal conditioned media). (**C**) GM-CSF/IL-4 treatment down-regulates CD14 expression on sDC in the presence of STAT3 Inhibitor IX Cpd188. (**i**) Representative dot plots without (left) and with (right) the STAT3 inhibitor. (**ii**) CD14 expression on day 3 DC (first bar) or sDC pre-treated with the STAT3 inhibitor (0, 0.5,1, 5, 10 μM) (mean + SEM; triplicates). (**D**) (**i**) Representative histogram; PD-L1 expression on day 5 DC or sDC (see above) treated with the STAT3 inhibitor (5μM Cpd188). (**ii**) Summary of the effect of the STAT3 inhibitor on PD-L1 expression. Bars represent the mean + SEM of PD-L1 expression on a single donor's DC or sDC, the latter treated with 50% PCaSt-CM from 3 different cultures (triplicates) in the presence (gray) or absence (black) of STAT3 inhibitor as in (**i**). (**E**). DC or sDC were cultured in the presence or absence of α-IL-6 and/or α-IL10 blocking antibodies (1 or 5 μg/mL) alone or together, for 5 d PD-L1 expression was assessed by flow cytometry. Mean + SEM from triplicate samples are shown. Statistical analysis was performed by two-way ANOVA; ns, not significant; ****$p < 0.0001$, ***$p < 0.001$, **$p < 0.01$, *$p < 0.05$.

Phenotypic analysis of $CD14^+$ cells among TIL as compared to those present among healthy donor PBMC revealed significantly higher levels of CD209 among tumor-associated $CD14^+$ lymphocytes (**Fig. 7B**). Furthermore, $CD14^+$ cells in TILs also expressed elevated levels of PD-L1, which was not the case in normal or patient PBMC, the latter obtained from the some of the same donors as the TIL (**Fig. 7C**). Furthermore, tumor-infiltrating T cells expressed elevated levels of PD-1 when compared to those among patient or healthy donor PBMC (**Fig. 7D**), implicating $PD\text{-}L1^+$ myeloid cells in the tumor microenvironment as suppressors of infiltrating T cells.

Taken together, our results provide strong evidence that the tumor stroma has a major influence on the behavior of myeloid cells in PCa, including the previously undescribed effect of the upregulation of PD-L1 by soluble stromal factors, with IL-6 a key contributor to this immunosuppressive phenotype.

Discussion

The precise immunoregulatory role of tumor-associated stroma, its influence on monocyte migration and myeloid cell-mediated contribution of an immunosuppressive tumor microenvironment in early PCa has been obscure. Using high purity primary stromal cultures, we demonstrate here that PCaSt attract monocytes via CCL2 secretion, and that stromal-derived factors affect monocyte to DC differentiation. Stromal factors are capable of inducing an immunosuppressive phenotype in DCs, characterized by the expression of $CD14^+/CD16^+/CD68^+/CD124^+/CD209^+$ and also by elevated expression of PD-L1. DC function is also affected by exposure to prostate cancer stroma conditioned media, such that we observed enhanced IL-10 production upon LPS stimulation, inhibition of T-cell responses and suboptimal tumor antigen cross-presenting ability, indicating complex immunosuppressive stromal activities in PCa.

Although the presence of $CD68^+$ myeloid cells in the prostate tumor microenvironment has been previously shown to correlate with increased risk of recurrence,[10] there is a paucity of detailed studies delineating the role of these myeloid cells. Migration of monocytes into tumor tissue is guided by tumor-derived soluble factors, most notably CCL2.[12,23] CCL2 can be produced by many cell types including epithelial, fibroblastic, endothelial and smooth muscle cells.[23] Its expression has been documented in prostate, breast, ovarian and colorectal cancers.[12,19,24-26] In early prostate cancers, we found that high levels of CCL2 were preferentially produced by the stroma rather than epithelial cells, and, this stromal CCL2 was responsible for driving monocyte migra-

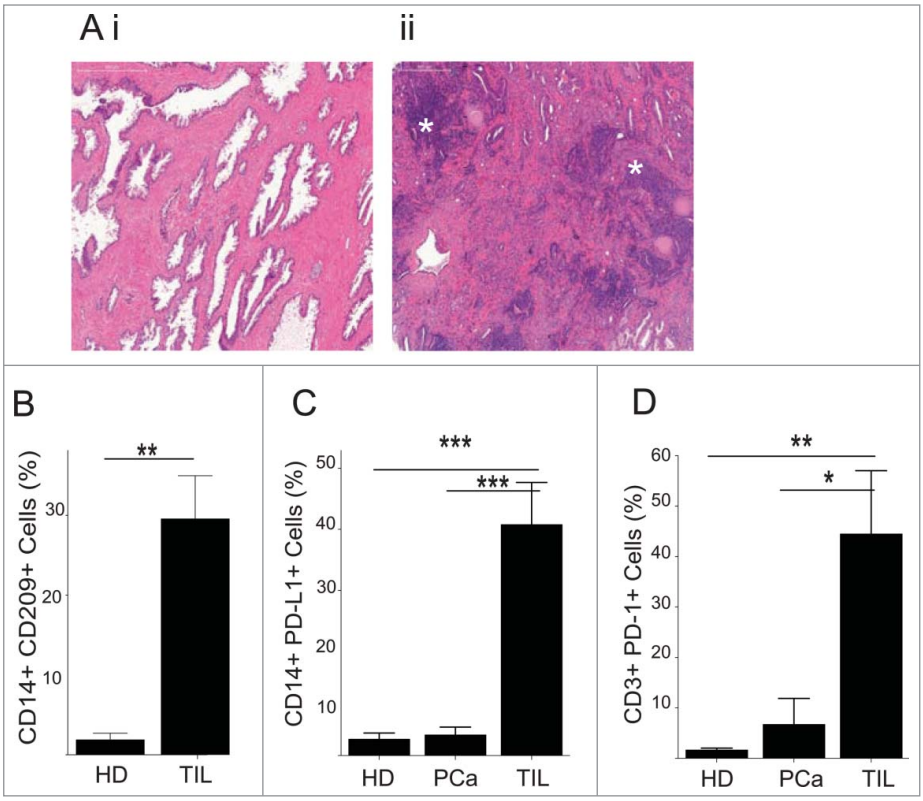

Figure 7. PD-L1 and CD209 expression on $CD14^+$ cells in prostate tumor tissue. Primary prostate cancer (PCa) tumor specimens were histologically examined (**A**) and isolated TILs from the malignant biopsies were phenotyped by immunostaining (**B–D**). (**A**) Tissue sections (4 μm) were stained with haematoxylin and eosin. Highly dense areas of infiltrating leukocytes present in the tumor (asterisks) (**ii**) but not in the normal tissue (**i**) (**B–D**) Fresh prostate biopsy tissue was homogenized and the phenotype of cells analyzed by flow cytometry. Mean + SEM of % positive cells from 3–7 different samples are shown. (**B**) The presence of $CD14^+CD209^+$ cells within tumor infiltrating leukocytes (TIL) (n = 3) and healthy donor blood (HD) (n = 6). **(C)** Programmed cell death ligand-1 (PD-L1) expression on $CD14^+$ cells from samples as in (B) and from PCa patient blood (PCa) (n = 7). (**D**) Programmed cell death-1 (PD-1) expression on $CD3^+$ T cells from samples as in (**C**). Statistical analysis was performed by unpaired Student's t-test; $^{****}p < 0.0001$, $^{***}p < 0.001$, $^{**}p < 0.01$, $^{*}p < 0.05$.

tion. CCL2 expression has been reported in PCaSt[12,14] although a recent study suggested that rather than CCL2, SDF-1α produced by tumor-associated fibroblasts is the driving force behind stromal-mediated monocyte migration.[27] However, in our study, little SDF-1 protein was detected in either PCaEp or PCaSt cultures. Blocking of CCL2 in PCaSt-CM, demonstrated a significant decrease in monocyte migration confirming the crucial role of CCL2. It is noteworthy that some CCL2 production by PCaEp was also detected, but it was significantly lower than the levels produced by PCaSt cells and migration of monocytes was not observed toward PCaEp-CM. CCL2 production was also observed by stromal cells that derived from the non-diseased areas of the prostate biopsy. Interestingly however, this did not seem to correlate with the differences in the frequencies of myeloid cells present in the diseased vs. normal areas of the prostate. We can only speculate that myeloid cells are retained better by the malignant tissue as a result of differential induction of adhesion molecules or chemokine receptors by cells within the tumor microenvironment.[28] Ongoing work in our laboratory is addressing the in depth differences between tumor vs. non-tumor prostate stroma. CCL2 is also known to activate $CD11b^+$ monocytes and enhance their IL-6 expression. IL-6 is among the inflammatory cytokines secreted by infiltrating cells in the tumor microenvironment, thereby reciprocally increasing CCL2 expression levels in the tissue. This can potentially result in an amplification loop that enhances monocyte infiltration, malignant cell proliferation and tumor survival.[29] In melanoma, TGFβ, which we have shown is also preferentially produced by stroma (as compared to epithelial cells) can also increase expression of CCL2 and IL-10, and enhance CCL2-dependent infiltration of monocytes followed by their differentiation into an immunosuppressive phenotype.[23] Our results provide evidence that tumor-associated stroma and not epithelia, in early PCa, has a dominant role in myeloid cell migration into the tumor microenvironment, which may represent an early microenvironmental event leading to immunosuppression.

GM-CSF and IL-4-induced monocyte differentiation to DC is skewed in the presence of PCaSt-CM and can be characterized by the failure of these cells to downregulate CD14 and by expressing the markers CD68/CD16/CD124/CD209, as well as the hallmark immune checkpoint regulatory protein, PD-L1. Among the soluble factors that we found present in the media of cultured stromal cells, IL-6 has been documented in many malignancies, including prostate, breast and colorectal cancers, and is often associated with poor prognosis.[30-32] IL-6 expression in PCa has been attributed to both stromal and tumor cells[33] and the influences of various tumor-derived factors, such as IL-6 and IL-10, on DC differentiation from myeloid cells have been previously studied.[34-37] Furthermore, tumor-derived soluble factors have also been shown to affect DC function,[38,39] Fibroblast-derived IL-6 has also previously been shown to effect the differentiation of monocytes into macrophages (rather than DCs).[40,41] However, our experiments clearly demonstrate that in early PCa, IL-6 expression is higher in PCaSt than PCaEp, indicating that stromal cells are the dominant cell type to influence myeloid cell differentiation. Furthermore, tumor-derived soluble factors exhibited a

significantly greater effect on the development of immunosuppressive DCs than factors derived from normal stroma, suggesting an altered milieu arising from reactive stroma.

Activated STAT3, a known mediator of tumor-associated inhibition of DC differentiation and function,[42,43] seemed crucial in our experiments such that inhibition of STAT3 restored CD14 downregulation during DC differentiation in the presence of PCaSt-CM. $CD14^+$ DC, generated by relatively high concentrations of IL-10 (40 ng/mL) *in vitro*, have been shown to express elevated levels of PD-L1.[44] However, in our experiments, <10 pg/mL IL-10 was detected in stroma CM and IL-10 was not induced by CM treatment above that induced by GM-CSF/IL-4, indicating that stromal factors other than IL-10 may contribute to PD-L1 upregulation on sDC. In hepatocellular carcinoma, autocrine IL-10 and tumor necrosis factor α (TNFα) induced by the tumor cell line supernatants have been shown to induce the expression of PD-L1 on monocytes.[45] We also demonstrate that blocking CM-induced STAT3 activation significantly inhibits the upregulation of PD-L1 on DCs. STAT3-dependent PD-L1 upregulation has been observed on liver plasmacytoid DCs[46] and on tolerogenic DCs, induced by early exposure to Toll-like receptor agonists.[47] To our knowledge, similar STAT3-dependent modulation of PD-L1 on DCs in response to tumor-stroma derived soluble factors has not been described before. We highlighted IL-6 as a significant contributor toward PD-L1 upregulation, although contribution by other factors has not yet been excluded. While neither TGFβ nor HGF alone did not appear to effect PD-L1 upregulation (data not shown), it is likely that the effect is due to a combination of several cytokines, the subject of ongoing studies.

Interaction between the receptor PD-1, expressed on T cells - especially in the tumor tissue, and its activating ligand PD-L1, exerts major effects on cytokine production by T cells and can also inhibit T-cell proliferation.[48] Tumors can evade immune eradication by exploiting the peripheral tolerance maintained through the binding of PD-1 and PD-L1.[48] Clinical trials targeting PD-1/PD-L1 (Nivolumab) are currently under way.[49,50] Our results highlight that PCaSt not only inhibits normal DC differentiation but may also regulate T-cell activity through PD-1/PD-L1. These observations support that Nivolumab may be advantageous in prostate cancer by preventing/removing microenvironmental immunosuppression.

In summary, our work demonstrates that in early PCa, stromal-derived factors alone are able to attract monocytes to the tumor microenvironment. In the presence of these stromal factors, monocytes are unable to differentiate into conventional DCs. The DCs arising from stromal regulation have an immunosuppressive phenotype, including increased expression of PD-L1. Thus, to our knowledge we convincingly show for the first time that primary tumor-associated stroma primarily exerts a negative influence on PCa disease progression by eliciting myeloid cell migration and altering their differentiation into fully functional DCs. These findings provide rationale for targeting tumor-associated stromal cells, which represent a potent immunosuppressive barrier to anticancer immunity, in order to facilitate the efficacy of cancer immunotherapies.

Materials and Methods

Tissue collection, isolation and expansion of primary prostate cells

Fresh PCa tissue was obtained from patients undergoing radical retropubic prostatectomy through the Wales Cancer Bank. Samples were obtained under informed consent and with ethical approval according to the Helsinki Declaration and institutional standards. Patients were histologically graded as having either Gleason 6 or 7 PCa by a certified histopathologist. Biopsies were taken from normal and diseased areas of the prostate by a pathologist and biopsy cores were subjected to mechanical homogenization followed by 200 U/mL collagenase-I digestion for 15–20h at 37°C. Primary PCaSt cultures were established and grown in Stromal Cell Basal Medium (SCBM) containing recombinant human fibroblast growth factor-B, insulin, fetal bovine serum (FBS) and GA-1000 (Lonza). Primary PCaEp cultures were established and grown in Keratinocyte Serum-Free Medium (K-SFM) containing recombinant epidermal growth factor 1–53 and bovine pituitary extract (Invitrogen). Conditioned media (CM) was generated by collecting the supernatants from PCaEp or PCaSt cultures 48 h after seeding at 1×10^5 cells/mL (referred to as PCaEp-CM and PCaSt-CM, respectively).

Cell lines

PCa cell lines (LNCaP and DU145) and HFF were purchased from the American Type Culture Collection. PCa cell lines were cultured in RPMI-1640 while HFFs in DMEM. Both media were supplemented with 10% FBS, 2 mM L-glutamine, 100 U/mL penicillin, 100 μg/mL streptomycin, 25 mM HEPES, 1 mM sodium-pyruvate. All cell lines were mycoplasma-free and were tested monthly.

Monocyte-derived dendritic cell culture

Venous blood was collected from healthy donors under informed consent and with ethical approval. PBMCs were separated by Histopaque (Sigma-Aldrich) density gradient centrifugation. Monocytes were separated either as untouched cells using the EasySep® Human Monocyte Enrichment kit without CD16 depletion (StemCell Technologies), in which case average purity of $CD14^+$ cells was approximately 82%, or by plastic adherence, with a purity of approximately 70–80%. Monocytes were cultured in SCBM containing 50 ng/mL recombinant human GM-CSF and 500 U/mL recombinant human IL-4. For soluble factor experiments, SCBM+50% PCaSt-CM or PCaEp-CM was added with GM-CSF/IL-4 as above. After 5 days, DC development was determined, based on downregulation of CD14 and upregulation of CD209 expression, by flow cytometry. Flow cytometry work was carried out on a FACSCanto or a FACSVerse flow cytometer (BD Biosciences) and the results were analyzed using FACSDiva (BD Biosciences) or FlowJo (TreeStar) software.

Immunofluorescence and immunocytochemistry

Indirect immunofluorescence was performed using antibodies for epithelial markers, CK5, CK8, CK14, CK18 and stromal

markers, α-SMA, vimentin and desmin (all from Santa Cruz Biotechnology). PCaEp and PCaSt were cultured until ~80% confluent. Prior to antibody staining, cells were fixed with ice-cold acetone:methanol (1:1) and blocked in 2% bovine serum albumin/7%Glycerol/PBS. Visualization of the cells was performed using a secondary goat anti-mouse Alexa488-conjugated antibody (Invitrogen). Samples were counterstained with 4′,6-diamidino-2-phenylindole (DAPI) and visualized using an Axiovert-40 fluorescence microscope (Zeiss). To quantify expression levels, cells were labeled with the same primary antibody but the secondary antibody was substituted for a goat anti-mouse biotin-conjugated antibody and streptavidin-conjugated europium. Bound europium was measured by time-resolved fluorescence on a Wallac Victor2 1420 plate reader (Perkin Elmer).

Paraffin embedded tissue staining

Formalin fixed paraffin embedded (FFPE) tissue sections were obtained from the same PCa patients as fresh tissue. Sections (4 μm) were dewaxed in xylene and rehydrated in 100% ethanol prior to staining with haematoxylin and eosin (H&E). Sections were mounted with DPX mounting solution and visualized on a Mirax scanner using the Pannoramic Viewing software (both 3D-Histech).

Cytokine array

To determine the secreted cytokine profiles, PCaEp-CM and PCaSt-CM were analyzed using the Proteome Profiler Human Cytokine Array Panel A kit (R&D Systems) according to the manufacturer's protocol.

Enzyme-linked immunosorbent assay

Quantitation of IFNγ, IL-12 and IL-10 was performed using Standard ELISA Development Kits (PeproTech) while measurements of TGFβ, HGF, VEGF and SDF-1 levels were performed using DuoSet ELISAs (R&D Systems). The detection step was performed using a europium-based detection method. After incubating with the biotinylated detection antibody, and followed by washing, 1 μg/mL europium-labeled streptavidin-conjugate (Perkin Elmer), diluted in DELFIA Assay Buffer, was added to each well and incubated at room temperature for 45 min. Following washing, 100 μL DELFIA Enhancement Solution (Perkin Elmer) was added to each well and incubated for 5 min at room temperature. Bound europium was measured as above.

Migration assays

Migration of monocytes was performed using 5 μm-pore size MilliCell Cell Culture Inserts (Millipore). MilliCell inserts containing 1×10^6 monocytes in 100 μL were placed into a 24-well plate containing 600 μL of either media alone or 10–50% PCaEp-CM or PCaSt-CM per well. Cells were left to migrate for 4 h prior to counting using the Millipore Guava® EasyCyteTM8 flow cytometer. CCL2 inhibition was performed by addition of 2 μg/mL neutralizing antibody (R&D Systems) to PCaSt-CM for 30 min prior to performing a migration assay. Recombinant human (rh) CCL2 was used at a range of 0.001–0.1 ng/mL to induce migration.

Flow cytometry

Cells were surface-labeled with fluorochrome-conjugated antibodies specific for CD3, CD14, CD15, CD16, CD11b, CD11c, CD1c, CD68, CD209, HLA-DR, PD-1 and PD-L1 (eBioscience). STAT3 phosphorylation was analyzed using fluorochrome-conjugated PhosFlow antibodies specific for STAT3 (pS727 and pY705) or isotype (BD Biosciences), following fixation and permeabilisation using 2% paraformaldehyde and 80% ice-cold methanol.

Mixed lymphocyte reaction (MLR)

DCs (10^4 cells/well) were cultured with allogeneic non-adherent PBMC (10^5 cells/well) in 96 well U-bottomed trays. [^{3}H]-Thymidine (GE Healthcare, Waukesha, WI) incorporation was measured after 3 days, with 0.5 μCi [^{3}H]-Thymidine/well added for the final 14 h of culture. Cells were harvested onto filtermats and counted in a Wallac 1450 MicroBeta- TriLux plate reader (PerkinElmer).

T-cell stimulation assay

DCs were cultured with CFSE-labeled autologous T cells at ratios of 1:50, 1:20 and 1:10. T-cell proliferation was induced by TCR cross-linking in cultures of 1×10^5 cells per well in 96-well U-bottom trays using CD3-CD28 antibody-coated beads (Dynal; Life Technologies) at a bead-to-cell ratio of 1:1 per well. Proliferation by CFSE dilution was measured by flow cytometry.

Antigen cross-presentation assay

DCs were incubated with 10 μg/mL 5T4 recombinant protein overnight. A $CD8^+$ T-cell line specific for a 5T4 peptide (RLARLALVL) was generated from a healthy HLA-$A2^+$ donor as described.[51] T cells were added to antigen-pulsed DCs at a 10:1 ratio and incubated for 24 h. IFNγ production was measured using ELISA, as described above. The negative control consisted of antigen-unpulsed DCs cultured with 5T4-specific T cells.

Phagocytosis assay

DCs (5×10^4) were incubated in 96-well culture trays with CFSE-labeled irradiated (30 Gy; ^{137}Cs-Source at 0.627 Gy/min) DU145 cells overnight at a 1:1 ratio. Cells were labeled with an allophycocyanin (APC)-conjugated HLA-DR antibody and phagocytosis was measured by calculating the percentage of double-positive cells by flow cytometry.

STAT3, IL-6 and IL-10 inhibition

Monocytes were cultured for 3 d in SCBM+50% PCaSt-CM, containing 50 ng/mL GM-CSF and 500 U/mL IL-4, and in the presence of varying concentrations (0.5–10 μM) of STAT3 Inhibitor IX Cpd188 (Millipore), dissolved in dimethyl sulfoxide (DMSO).[52] CD14, CD209 and PD-L1 expression was measured by flow cytometry. IL-6 and IL-10 neutralizing antibodies and isotype controls were obtained from eBioscience. Monocytes were cultured as above for 5 d in the presence or absence of 1 or 5 μg/mL of the neutralizing antibodies, as indicated, for 5 d when phenotyping was carried out.

Statistical analysis

Unless otherwise indicated, statistical analysis was performed by two-way ANOVA.

Disclosure of Potential Conflicts of Interest

No potential conflicts of interest were disclosed.

Acknowledgments

We thank the Wales Cancer Bank for patient samples and Ms Lynda Churchill for technical assistance.

Funding

This study was supported by a program grant from Cancer Research Wales to ZT, AC and MDM.

References

1. Hanahan D, Weinberg RA. Hallmarks of cancer: the next generation. Cell 2011; 144:646-74; PMID:21376230; http://dx.doi.org/10.1016/j.cell.2011.02.013
2. Karja V, Aaltomaa S, Lipponen P, Isotalo T, Talja M, Mokka R. Tumour-infiltrating lymphocytes: A prognostic factor of PSA-free survival in patients with local prostate carcinoma treated by radical prostatectomy. Anticancer Res 2005; 25:4435-8.
3. Karan D, Holzbeierlein JM, Van Veldhuizen P, Thrasher JB. Cancer immunotherapy: a paradigm shift for prostate cancer treatment. Nat Rev Urol 2012; 9:376-85; PMID:22641164; http://dx.doi.org/10.1038/nrurol.2012.106
4. Miller AM, Pisa P. Tumor escape mechanisms in prostate cancer. Cancer Immunol Immunother 2007; 56:81-7; PMID:16362411; http://dx.doi.org/10.1007/s00262-005-0110-x
5. Peehl DM. Primary cell cultures as models of prostate cancer development. Endocr Relat Cancer 2005; 12:19-47; PMID:15788637; http://dx.doi.org/10.1677/erc.1.00795
6. Allavena P, Sica A, Solinas G, Porta C, Mantovani A. The inflammatory micro-environment in tumor progression: the role of tumor-associated macrophages. Crit Rev Oncol Hematol 2008; 66:1-9; PMID:17913510; http://dx.doi.org/10.1016/j.critrevonc.2007.07.004
7. Ostrand-Rosenberg S, Sinha P. Myeloid-derived suppressor cells: linking inflammation and cancer. J Immunol 2009; 182:4499-506; PMID:17913510; http://dx.doi.org/10.4049/jimmunol.0802740
8. Vuk-Pavlovic S, Bulur PA, Lin Y, Qin R, Szumlanski CL, Zhao X, Dietz AB. Immunosuppressive CD14+HLA-DRlow- monocytes in prostate cancer. Prostate 2010; 70:443-55; PMID:19902470; http://dx.doi.org/10.1002/pros.21078
9. Troy A, Davidson P, Atkinson C, Hart D. Phenotypic characterisation of the dendritic cell infiltrate in prostate cancer. J Urol 1998; 160:214-9; http://dx.doi.org/10.1016/S0022-5347(01)63093-3
10. Gannon PO, Poisson AO, Delvoye N, Lapointe R, Mes-Masson AM, Saad F. Characterization of the intra-prostatic immune cell infiltration in androgen-deprived prostate cancer patients. J Immunol Methods 2009; 348:9-17; PMID:19552894; http://dx.doi.org/10.1016/j.jim.2009.06.004
11. Lindholm PF, Lu Y, Adley BP, Vladislav T, Jovanovic B, Sivapurapu N, Yang XJ, Kajdacsy-Balla A. Role of monocyte-lineage cells in prostate cancer cell invasion and tissue factor expression. Prostate 2010; 70:1672-82; PMID:20607747; http://dx.doi.org/10.1002/pros.21202
12. Loberg RD, Ying C, Craig M, Yan L, Snyder LA, Pienta KJ. CCL2 as an important mediator of prostate cancer growth in vivo through the regulation of macrophage infiltration. Neoplasia 2007; 9:556-62; PMID:17710158; http://dx.doi.org/10.1593/neo.07307
13. Taichman RS, Cooper C, Keller ET, Pienta KJ, Taichman NS, McCauley LK. Use of the stromal cell-derived factor-1CXCR4 pathway in prostate cancer metastasis to bone. Cancer Res 2002; 62:1832-7; PMID:11912162
14. Loberg RD, Day LL, Harwood J, Ying C, St John LN, Giles R, Neeley CK, Pienta KJ. CCL2 is a potent regulator of prostate cancer cell migration and proliferation. Neoplasia 2006; 8:578-86; PMID:16867220; http://dx.doi.org/10.1593/neo.06280
15. Tuxhorn JA, Ayala GE, Smith MJ, Smith VC, Dang TD, Rowley DR. Reactive stroma in human prostate cancer: induction of myofibroblast phenotype and extracellular matrix remodeling. Clin Cancer Res 2002; 8:2912-23; PMID:12231536
16. Herrera M, Herrera A, Dominguez G, Silva J, Garcia V, Garcia JM, Gomez I, Soldevilla B, Munoz C, Provencio M, et al. Cancer-associated fibroblast and M2 macrophage markers together predict outcome in colorectal cancer patients. Cancer Sci 2013; 104:437-44; PMID:23298232; http://dx.doi.org/10.1111/cas.12096
17. Medrek C, Ponten F, Jirstrom K, Leandersson K. The presence of tumor associated macrophages in tumor stroma as a prognostic marker for breast cancer patients. BMC Cancer 2012; 12:306; PMID:22824040; http://dx.doi.org/10.1186/1471-2407-12-306
18. Santoni M, Massari F, Amantini C, Nabissi M, Maines F, Burattini L, Berardi R, Santoni G, Montironi R, Tortora G, et al. Emerging role of tumor-associated macrophages as therapeutic targets in patients with metastatic renal cell carcinoma. Cancer Immunol Immunother 2013; 62:1757-68; PMID:24132754; http://dx.doi.org/10.1007/s00262-013-1487-6
19. Sanford DE, Belt BA, Panni RZ, Mayer A, Deshpande AD, Carpenter D, Mitchem JB, Plambeck-Suess SM, Worley LA, Goetz BD, et al. Inflammatory monocyte mobilization decreases patient survival in pancreatic cancer: a role for targeting the CCL2CCR2 axis. Clin Cancer Res 2013; 19:3404-15; PMID:23653148; http://dx.doi.org/10.1158/1078-0432.CCR-13-0525
20. Zou W, Chen L. Inhibitory B7-family molecules in the tumour microenvironment. Nat Rev Immunol 2008; 8:467-77; PMID:18500231; http://dx.doi.org/10.1038/nri2326
21. Southall PJ, Boxer GM, Bagshawe KD, Hole N, Bromley M, Stern PL. Immunohistological distribution of 5T4 antigen in normal and malignant tissues. Br J Cancer 1990; 61:89-95; PMID:2404511; http://dx.doi.org/10.1038/bjc.1990.20
22. Sumpter TL, Thomson AW. The STATus of PD-L1 (B7-H1) on tolerogenic APCs. Eur J Immunol 2011; 41:286-90; PMID:21267998; http://dx.doi.org/10.1002/eji.201041353
23. Deshmane SL, Kremlev S, Amini S, Sawaya BE. Monocyte chemoattractant protein-1 (MCP-1): an overview. J Interferon Cytokine Res 2009; 29:313-26; PMID:19441883; http://dx.doi.org/10.1089/jir.2008.0027
24. Fujimoto H, Sangai T, Ishii G, Ikehara A, Nagashima T, Miyazaki M, Ochiai A. Stromal MCP-1 in mammary tumors induces tumor-associated macrophage infiltration and contributes to tumor progression. Int J Cancer 2009; 125:1276-84; PMID:19479998; http://dx.doi.org/10.1002/ijc.24378
25. Negus RP, Stamp GW, Relf MG, Burke F, Malik ST, Bernasconi S, Allavena P, Sozzani S, Mantovani A, Balkwill FR. The detection and localization of monocyte chemoattractant protein-1 (MCP-1) in human ovarian cancer. J Clin Invest 1995; 95:2391-6; PMID:7738202; http://dx.doi.org/10.1172/JCI117933
26. Bailey C, Negus R, Morris A, Ziprin P, Goldin R, Allavena P, Peck D, Darzi A. Chemokine expression is associated with the accumulation of tumour associated macrophages (TAMs) and progression in human colorectal cancer. Clin Exp Metastasis 2007; 24:121-30; PMID:17390111; http://dx.doi.org/10.1007/s10585-007-9060-3
27. Comito G, Giannoni E, Segura CP, Barcellos-de-Souza P, Raspollini MR, Baroni G, Lanciotti M, Serni S, Chiarugi P. Cancer-associated fibroblasts and M2-polarized macrophages synergize during prostate carcinoma progression. Oncogene 2014; 33:2423-31; PMID:23728338; http://dx.doi.org/10.1038/onc.2013.191
28. Franklin RA, Liao W, Sarkar A, Kim MV, Bivona MR, Liu K, Pamer EG, Li MO. The cellular and molecular origin of tumor-associated macrophages. Science 2014; 344:921-5; PMID:24812208; http://dx.doi.org/10.1126/science.1252510
29. Roca H, Varsos ZS, Sud S, Craig MJ, Ying C, Pienta KJ. CCL2 and interleukin-6 promote survival of human CD11b+ peripheral blood mononuclear cells and induce M2-type macrophage polarization. J Biol Chem 2009; 284:34342-54; PMID:19833726; http://dx.doi.org/10.1074/jbc.M109.042671
30. Nakashima J, Tachibana M, Horiguchi Y, Oya M, Ohigashi T, Asakura H, Murai M. Serum interleukin 6 as a prognostic factor in patients with prostate cancer. Clin Cancer Res 2000; 6:2702-6; PMID:10914713
31. Zhang GJ, Adachi I. Serum interleukin-6 levels correlate to tumor progression and prognosis in metastatic breast carcinoma. Anticancer Res 1999; 19:1427-32; PMID:10365118
32. Chung YC, Chang YF. Serum interleukin-6 levels reflect the disease status of colorectal cancer. J Surg Oncol 2003; 83:222-6; PMID:12884234; http://dx.doi.org/10.1002/jso.10269
33. Hobisch A, Rogatsch H, Hittmair A, Fuchs D, Bartsch G, Jr., Klocker H, Bartsch G, Culig Z. Immunohistochemical localization of interleukin-6 and its receptor in benign, premalignant and malignant prostate tissue. J Pathol 2000; 191:239-44; PMID:10878544; http://dx.doi.org/10.1002/1096-9896(2000)9999:9999%3c::AID-PATH633%3e3.0.CO;2-X
34. van de Ven R, Lindenberg JJ, Oosterhoff D, de Gruijl TD. Dendritic Cell Plasticity in Tumor-Conditioned Skin: CD14(+) Cells at the Cross-Roads of Immune Activation and Suppression. Frontiers in immunology 2013; 4:403.
35. Chen F, Hou M, Ye F, Lv W, Xie X. Ovarian cancer cells induce peripheral mature dendritic cells to differentiate into macrophagelike cells in vitro. Int J Gynecol Cancer 2009; 19:1487-93; PMID:19955923; http://dx.doi.org/10.1111/IGC.0b013e3181bb70c6
36. Figel AM, Brech D, Prinz PU, Lettenmeyer UK, Eckl J, Turqueti-Neves A, Mysliwietz J, Anz D, Rieth N, Muenchmeier N, et al. Human renal cell carcinoma induces a dendritic cell subset that uses T-cell crosstalk for tumor-permissive milieu alterations. Am J Pathol 2011; 179:436-51; PMID:21703422; http://dx.doi.org/10.1016/j.ajpath.2011.03.011
37. Heusinkveld M, de Vos van Steenwijk PJ, Goedemans R, Ramwadhdoebe TH, Gorter A, Welters MJ, van Hall T, van der Burg SH. M2 macrophages induced by prostaglandin E2 and IL-6 from cervical carcinoma are switched to activated M1 macrophages by CD4+ Th1 cells. J Immunol 2011; 187:1157-65; PMID:21709158; http://dx.doi.org/10.4049/jimmu-nol.1100889
38. Ramanathapuram LV, Hopkin D, Kurago ZB. Dendritic Cells (DC) Facilitate Detachment of Squamous

Carcinoma Cells (SCC), While SCC Promote an Immature CD16(+) DC Phenotype and Control DC Migration. Cancer Microenviron 2013; 6:41-55; PMID:21809059; http://dx.doi.org/10.1007/s12307-011-0077-4

39. Diao J, Mikhailova A, Tang M, Gu H, Zhao J, Cattral MS. Immunostimulatory conventional dendritic cells evolve into regulatory macrophage-like cells. Blood 2012; 119:4919-27; PMID:22490680; http://dx.doi.org/10.1182/blood-2011-11-392894
40. Chomarat P, Banchereau J, Davoust J, Palucka AK. IL-6 switches the differentiation of monocytes from dendritic cells to macrophages. Nat Immunol 2000; 1:510-4; PMID:11101873; http://dx.doi.org/10.1038/82763
41. Dominguez-Soto A, Sierra-Filardi E, Puig-Kroger A, Perez-Maceda B, Gomez-Aguado F, Corcuera MT, Sanchez-Mateos P, Corbi AL. Dendritic cell-specific ICAM-3-grabbing nonintegrin expression on M2-polarized and tumor-associated macrophages is macrophage-CSF dependent and enhanced by tumor-derived IL-6 and IL-10. J Immunol 2011; 186:2192-200; PMID:21239715; http://dx.doi.org/10.4049/jimmunol.1000475
42. Yu H, Kortylewski M, Pardoll D. Crosstalk between cancer and immune cells: role of STAT3 in the tumour microenvironment. Nat Rev Immunol 2007; 7:41-51; PMID:17186030; http://dx.doi.org/10.1038/nri1995
43. Oosterhoff D, Lougheed S, van de Ven R, Lindenberg J, van Cruijsen H, Hiddingh L, Kroon J, van den Eertwegh AJ, Hangalapura B, Scheper RJ, et al. Tumor-mediated inhibition of human dendritic cell differentiation and function is consistently counteracted by combined p38 MAPK and STAT3 inhibition. Oncoimmunology 2012; 1:649-58; PMID:22934257; http://dx.doi.org/10.4161/onci.20365
44. Lindenberg JJ, van de Ven R, Lougheed SM, Zomer A, Santegoets SJ, Griffioen AW, Hooijberg E, van den Eertwegh AJ, Thijssen VL, Scheper RJ, et al. Functional characterization of a STAT3-dependent dendritic cell-derived CD14 cell population arising upon IL-10-driven maturation. Oncoimmunology 2013; 2:e23837; PMID:23734330; http://dx.doi.org/10.4161/onci.23837
45. Kuang DM, Zhao Q, Peng C, Xu J, Zhang JP, Wu C, Zheng L. Activated monocytes in peritumoral stroma of hepatocellular carcinoma foster immune privilege and disease progression through PD-L1. J Exp Med 2009; 206:1327-37; PMID:19451266; http://dx.doi.org/10.1084/jem.20082173
46. Matta BM, Raimondi G, Rosborough BR, Sumpter TL, Thomson AW. IL-27 production and STAT3-dependent upregulation of B7-H1 mediate immune regulatory functions of liver plasmacytoid dendritic cells. J Immunol 2012; 188:5227-37; PMID:22508931; http://dx.doi.org/10.4049/jimmunol.1103382
47. Wolfle SJ, Strebovsky J, Bartz H, Sahr A, Arnold C, Kaiser C, Dalpke AH, Heeg K. PD-L1 expression on tolerogenic APCs is controlled by STAT-3. Eur J Immunol 2011; 41:413-24; PMID:21268011; http://dx.doi.org/10.1002/eji.201040979
48. Riella LV, Paterson AM, Sharpe AH, Chandraker A. Role of the PD-1 pathway in the immune response. Am J Transplant 2012; 12:2575-87; PMID:22900886; http://dx.doi.org/10.1111/j.1600-6143.2012.04224.x
49. Aranda F, Vacchelli E, Eggermont A, Galon J, Fridman WH, Zitvogel L, Kroemer G, Galluzzi L. Trial Watch: Immunostimulatory monoclonal antibodies in cancer therapy. Oncoimmunology 2014; 3:e27297; PMID:24701370; http://dx.doi.org/10.4161/onci.27297
50. Taube JM, Klein AP, Brahmer JR, Xu H, Pan X, Kim JH, Chen L, Pardoll DM, Topalian SL, Anders RA. Association of PD-1, PD-1 ligands, and other features of the tumor immune microenvironment with response to anti-PD-1 therapy. Clin Cancer Res 2014; PMID:24714771; Epub: 8 April 2014.
51. Al-Taei S, Salimu J, Lester JF, Linnane S, Goonewardena M, Harrop R, Mason MD, Tabi Z. Overexpression and potential targeting of the oncofoetal antigen 5T4 in malignant pleural mesothelioma. Lung Cancer 2012; 77:312-8; PMID:22498111; http://dx.doi.org/10.1016/j.lungcan.2012.03.008
52. Xu X, Kasembeli MM, Jiang X, Tweardy BJ, Tweardy DJ. Chemical probes that competitively and selectively inhibit Stat3 activation. PLoS One 2009; 4:e4783; PMID:19274102; http://dx.doi.org/10.1371/journal.pone.0004783